Nonlocal voltage effects in $La_{2/3}Ca_{1/3}MnO_3/La_{1/3}Ca_{2/3}MnO_3/YBa_2Cu_3O_7$ trilayers

M. Cuoco,[1,2] W. Saldarriaga,[3] A. Polcari,[1,4] A. Guarino,[1,2] O. Moran,[3] E. Baca,[5] A. Vecchione,[1,2] and P. Romano[1,4]
[1]*Laboratorio Regionale SuperMat, CNR-INFM Salerno, Baronissi (Sa), Italy*
[2]*Dipartimento di Fisica "E.R. Caianiello," Universitá di Salerno, Baronissi (Sa), Italy*
[3]*Departamento de Física, Laboratorio de Materiales Cerámicos y Vítreos, Universidad Nacional de Colombia sede Medellín, A.A. 568 Medellín, Colombia*
[4]*Dipartimento di Scienze Biologiche ed Ambientali, Via Port'Arsa 11, Universitá del Sannio, I-82100 Benevento, Italy*
[5]*Departamento de Física, Grupo de Ingenieria de Nuevos Materiales, Universidad del Valle, A.A. 25360 Cali, Colombia*
(Received 15 May 2008; revised manuscript received 4 December 2008; published 30 January 2009)

We consider nonlocal conductance effects in epitaxial trilayers made by ferromagnetic half-metal $La_{2/3}Ca_{1/3}MnO_3$ and high T_c superconductor $YBa_2Cu_3O_{7-\delta}$ separated by an insulating barrier of antiferromagnetic $La_{1/3}Ca_{2/3}MnO_3$ with variable thickness. The Hall transresistance as a function of the barrier thickness and the applied magnetic field is measured to investigate the interplay between tunneling and frictional drag effects in ferromagnet/antiferromagnet/superconductor trilayers. The results show a subtle correlation between the tunneling and the drag to account for the observed decreasing of the transresistance as the barrier thickness and the magnetic field are varied. A phenomenological model addresses such features as an enhancement of the frictional drag when the process of tunneling gets suppressed.

DOI: 10.1103/PhysRevB.79.014523 PACS number(s): 74.50.+r, 74.72.Bk, 74.78.Fk, 72.25.Mk

I. INTRODUCTION

Ferromagnetic/superconducting (FM/SC) heterostructures are at the center of intense theoretical and experimental investigation as they exhibit a wide class of complex phenomena and unconventional effects.[1,2] Among the various possibilities, FM/SC systems can manifest distinct features as: spin-mixing effects inducing spin-triplet pairing correlations at the interface,[3] Josephson couplings between two singlet-superconducting layers separated by a half-metallic ferromagnet,[4,5] oscillations in the singlet pairing amplitude detected in SC/FM/SC geometries,[6,7] and magnetic exchange coupling in FM/SC/FM geometries.[8,9] Since transition-metal oxides have similar lattice spacings, the combination of colossal magnetoresistance (CMR) manganites and high-T_c cuprates has been specially investigated. Experimental results suggest a strong FM/SC interplay resulting in the injection of spin-polarized carriers into the SC layers.

In this work, we have analyzed the transport properties of a trilayer system made by a ferromagnetic half-metal $La_{2/3}Ca_{1/3}MnO_3$ (LCMO-F) and a high T_c superconductor $YBa_2Cu_3O_{7-\delta}$ (YBCO) separated by an insulating barrier of antiferromagnetic $La_{1/3}Ca_{2/3}MnO_3$ (LCMO-AF). We focus on the charge imbalance induced on the ferromagnetic subsystem by a drive current flowing through the superconducting side and vice versa. The origin of such characteristics of nonlocal resistance can be related both to drag effects in conventional superconductor/normal junctions as well as to crossed Andreev reflection, elastic cotunneling, or charge imbalance in SC/FM systems within a three terminal geometry.[10,11] Here, our interest is devoted to the modification of the effective transresistance by tuning either the junction barrier or by applying an external magnetic field.

The structural characterization of the trilayers has been done by x-ray diffraction analysis, revealing a highly epitaxial heterostructure with well defined interfaces for all the studied samples. For the transport analysis, our measurements have been performed in a cross configuration with the aim of extracting the behavior of the nonlocal Hall transresistance as the barrier thickness and an applied magnetic field are varied (see Fig. 1). The resistance is nonlocal in the sense that the voltage is measured in a region where there is no drive current. Here, the transresistance $R_{\alpha/\beta}$ is given by

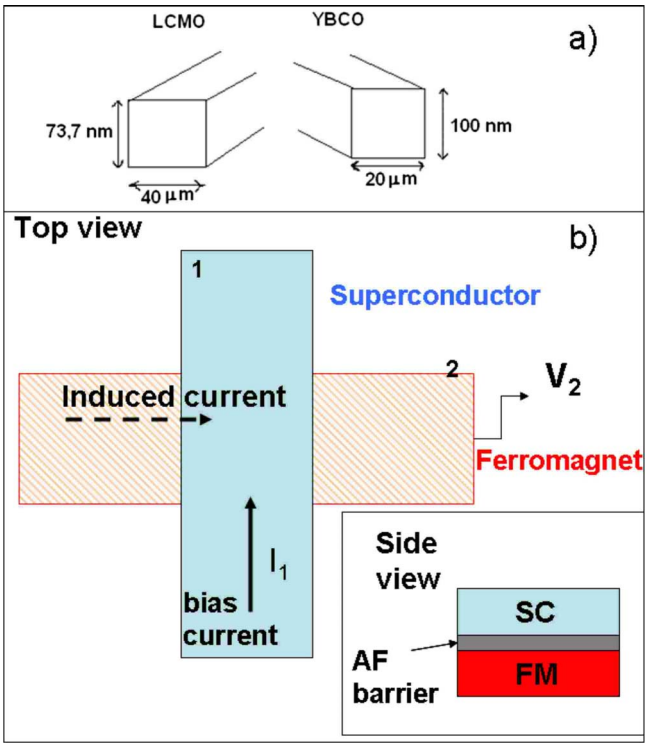

FIG. 1. (Color online) (a) indicates schematically the width and the height of YBCO and LCMO strips. (b) Sketch of the trilayer system indicating the drive or induced current as well as the applied or induced voltage configurations. FM and SC stand for ferromagnetic and superconducting films, respectively.

the ratio between the induced voltage V_α and the drive current I_β with contacts on α=LCMO[YBCO] and β=YBCO[LCMO], respectively.

General features may be extracted from the present investigation. (1) A finite transresistance can be detected in zero field for the case of a bias current on the superconductor I_{YBCO} and a voltage drop at the edge of the ferromagnet V_{LCMO}. (2) The result is not symmetric if one exchanges the contacts for the drive current and the potential difference, i.e., I_{LCMO} and V_{YBCO}, because in such configuration, a voltage at the edge of the YBCO is induced by a current drive through the LCMO only if the current overcomes a critical threshold. (3) $R_{LCMO/YBCO}$ decreases both as a function of the barrier thickness and of the applied magnetic field. Within a simple phenomenological model that includes both effects due to tunneling (charge transfer) and drag conductance, it is possible to interpret the result (3) as a reduction in the tunneling contribution with respect to the drag if the barrier thickness or the magnetic field grows in amplitude.

The paper is organized as follows. In Sec. II, we report about the structural analysis performed by x-ray diffraction on different trilayers having unequal barrier thickness. Section III is devoted to the presentation of the results about the nonlocal resistance as a function of the barrier thickness and the applied magnetic field as measured in the cross configuration shown in Fig. 1. Hence, in Sec. IV we discuss the results obtained in the light of the possible coupling mechanism between the superconductor and the ferromagnet in terms of tunneling and drag contribution for the nonlocal conductance. Finally, Sec. V is devoted to the concluding remarks.

II. SAMPLES FABRICATION AND STRUCTURAL CHARACTERIZATION

Trilayer structures composed by YBCO/LCMO-AF(d)/LCMO-F with d=3.7, 6.2, and 8.6 nm have been successfully fabricated and characterized. Hereafter, we will refer to them as samples 3, 5, and 7 (these numbers indicate the duration in minutes for each barrier LCMO-AF deposition).

The junctions were grown on [001] substrates using dc sputtering. The fabrication started with the deposition of a 73.7 nm thick base ferromagnetic (FM) layer onto a $SrTiO_3$ (STO) substrate at pure oxygen atmosphere with a pressure of 3.5 mbar, a dc power of 30 W, and a substrate temperature of about 1123 K. After the deposition the film was slowly cooled to 300 K in an atmosphere of 600 mbar. The junction area was defined by using standard lithographic techniques. First, the basis FM layer was patterned to 40 μm wide microbridge by using a chemical etching process based on a H_2SO_4 solution. Subsequently, after masking the FM strip edges, the antiferromagnetic (AF) layers with thicknesses of 3.7, 6.2, and 8.6 nm and the superconducting ones of 100 nm were grown upon this strip by dc sputtering under the same deposition parameters. Only for the deposition of the superconducting layers, the dc power was increased to 34 W. After slowly cooling down to 300 K in the same atmosphere, as before the sample was taken out of the chamber and then the

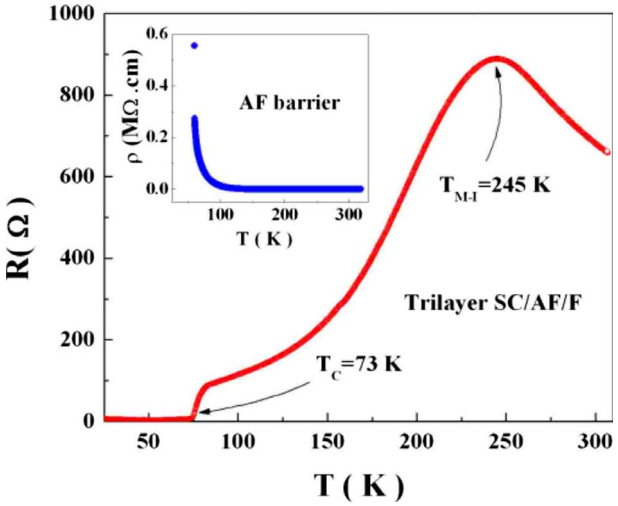

FIG. 2. (Color online) Temperature dependence of the resistance for the trilayers system with the contact configuration on the superconducting side. The inset indicates the resistivity for the individual barrier component grown on the $SrTiO_3$ substrate. T_c is the superconducting critical temperature, T_{M-I} denotes the temperature for the metal-insulator crossover in the LCMO component.

junction was completed by patterning a 20 μm wide strip on the top electrode (SC layer) by means of a H_3PO_4 solution. Since the H_3PO_4 etching solution is highly selective for SC material without affecting the AF layer, the presence of a SC/AF/FM junction with an area of 20×40 μm^2 is guaranteed.

The critical current density $J_c=I_c$/(transversal section) of YBCO films can be obtained by inspection of the injection I-V curves as reported in Ref. 12. The estimated critical current at 15 K is about 14 mA. Then, considering that the transversal section (i.e., the thickness times the width of the film) is about 2 μm^2, the amplitude of the critical current density is $J_c=7\times10^5$ A/cm^2.

At this point it is worth pointing out that concerning the possibilities of spurious contacts, the procedure used for the fabrication should not lead to leakages along the edges of the system because the AF part is covering the FM layers and the second etching removes only the superconducting YBCO component. Nevertheless, intrinsic roughness of the ceramic constituents of the device represents a major limit for the realization of junctions with sharp interfaces. Indeed, analysis on the surface of YBCO, LCMO-AF, and LCMO-FM films have revealed the presence of a root-mean-square surface roughness of about 2 nm which in turn may hamper a reliable and reproducible growing of the artificial barriers.[12] As a consequence, the ultrathin barriers may be affected by the presence of pinholes concentration that contribute to the tunneling from the FM to the SC layer.[12] Hence, pinholes in the barrier cannot be completely ruled out. Such effect will be considered in the analysis of Sec. IV.

As one can see in Fig. 2, the antiferromagnetic layer (LCMO-AF) is electrically insulating at low temperatures and constitutes a separation barrier between the superconducting YBCO and the ferromagnetic (with Curie temperature at 245 K) electrically normal-metal LCMO-F. In our

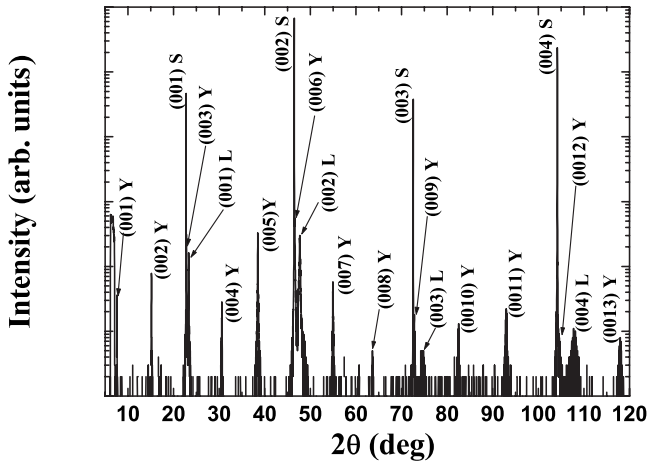

FIG. 3. $2\theta-\omega$ scan of sample 3. Only $(00l)$ reflections for YBCO (y) and LCMO (l), as expected on a $SrTiO_3$ (001) oriented substrate (s).

samples, the T_c of YBCO single layer when grown on STO is 86 K, while it decreases to about 73 K inside the trilayers (Fig. 2).

The structural analyses were carried out by high-resolution x-ray diffraction patterns obtained using a Philips X-Pert MRD diffractometer. Monochromatic Cu $K\alpha_1$ radiation (with wavelength $\lambda=0.154\,056$ nm) was obtained equipping the diffractometer with a four-crystal Ge (220) asymmetric monochromator and a graded parabolic mirror positioned on the primary arm which reduces the incident-beam divergence to 0.12 arc sec. A special sample holder allows to tilt the specimen (ψ angle) while rotating it in its own plane around an axis normal to its surface (ϕ angle). The first movement changes the ψ angle from $-90°$ to $90°$, whereas the second one changes the ϕ angle from $0°$ to $360°$. Moreover, it is possible to vary the angle of incidence, ω, of the x rays on the surface of the samples.

The structural data are discussed by assuming a cubic perovskite structure for the STO with $a_S=0.3905$ nm. As an example, Fig. 3 gives a $2\theta-\omega$ measurement performed on sample 3 in the range $5°<2\theta<120°$, showing only $(00l)$ reflections for YBCO, LCMO, and STO. This pattern indicates that all the layers are oriented with the c axis perpendicular to the surface of the substrate. No presence of spurious phases was revealed. From the patterns analysis, only a series of $(00l)$ reflections have been detected and attributed to LCMO layers. Similar results have been obtained in all the analyzed samples.

The thicknesses of the YBCO and LCMO layers were evaluated by the Debye-Scherrer formula. The obtained values are in agreement with those estimated by films deposition rates, i.e., $d_{\mathrm{YBCO}}\simeq 100$ nm and $d_{\mathrm{LCMO}}\simeq 150$ nm, respectively.

An epitaxial thin film grows on top of another film or substrate under in-plane compressive or tensile strain given by $\epsilon=(\sqrt{a_b b_b}-\sqrt{a_t b_t})/\sqrt{a_t b_t}$ where the subscripts b and t specify bottom and top bulk (unstressed) values of the layers, respectively. By growing directly on STO, the YBCO layer is expected to be in-plane biaxially tensile strained while the out-of-plane c axis is compressed. In order to evaluate the lattice parameters of the YBCO and LCMO layers, two extra Bragg reflections were measured, selecting the appropriate values for ϕ and ψ angles in the 2θ-ω scans. Our measurements show that YBCO layer is relaxed, with an orthorhombic crystal structure as expected for a superconducting sample.

For all the measured samples, the out-of-plane lattice parameter attributed to the LCMO compound is shorter than the bulk value for the LCMO-F phase whereas it is larger than the expected for the LCMO-AF one.[13] However, if one takes into account the values of the lattice parameters and the thicknesses of LCMO layers deposited during the sputtering process, it is expected to distinguish between the two LCMO phases. The experimental result was then interpreted considering the measured reflections as due to a superimposition of the LCMO-F and LCMO-AF phases. In this framework being the LCMO-AF very thin, it does not relax the tensile strain imposed by the overlying YBCO layer. As a consequence, the strain imposed on LCMO-F which is expected to be compressive ($\epsilon>0$) when deposited on LCMO-AF becomes tensile ($\epsilon<0$). Then, the measured lattice parameter c takes a single value resulting from the YBCO/LCMO-AF and LCMO-AF/LCMO-F strain processes for all the measured samples.

To further monitor the lattice mismatch between YBCO and STO as well as between LCMO and YBCO, reciprocal space maps have been carried out on symmetric $(00l)$ and asymmetric $(h0l)$ reflections. Naming d the interplanar spacing between reflecting crystalline planes, the modulus of the scattering vector can be defined as $|\mathbf{Q}|=2\pi/d$. Using the Bragg law, one can have $|\mathbf{q}|=|\mathbf{Q}|/2\pi=(2/\lambda)\sin\theta$.

In our reciprocal space maps, q_x and q_z represent the projections of the scattering vector in the plane identified by parallel and orthogonal axes to the surface of the substrate, that overlap with $[100]^*$ and $[001]^*$ directions, respectively. In particular, one can show that

$$\mathbf{q_x}=R[\cos\omega-\cos(2\theta-\omega)],$$

$$\mathbf{q_z}=R[\sin\omega+\sin(2\theta-\omega)],$$

where $R=1/2$ is the Ewald sphere radius and the reciprocal-lattice unit is defined as $\lambda/2d$.[14] As an example of mapping on symmetric reflections, the reciprocal space map containing the (002) reflection of both the LCMO layers and STO and (006) of the YBCO layer for sample 3 is reported in Fig. 4(a). The measurements confirm a good out-of-plane alignment for the STO, YBCO, and LCMO c axes. Figure 4(b) shows the asymmetric map of the reflections (103) for LCMO and STO and (109) for YBCO within the reciprocal space. The peaks are shifted from the expected position for the bulk compounds, as a consequence of the strains imposed on the different layers. From the asymmetric map an elongation in the q_x coordinate can be noticed for YBCO layer due to the in-plane lattice mismatch relaxation between YBCO and STO. This shows a tendency toward a reduction in tensile strain imposed by STO on YBCO with increasing thickness. Moreover, the asymmetric map shows only a (103) reflection coming from LCMO layers, confirming that the contributions of the ferromagnetic and the antiferromagnetic

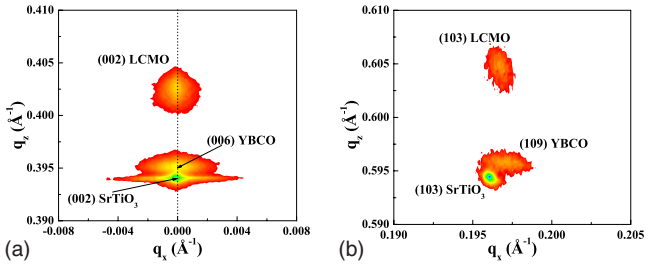

FIG. 4. (Color online) (a) Symmetric reciprocal space map of sample 3. The out-of-plane reflections of the layers are perfectly aligned with the (002) of the STO. (b) Asymmetric reciprocal space map of sample 3. Selected reflections in the (*h*0*l*) plane confirm a good alignment of all the layers also in plane.

layers are superimposed to give a single spot. All the analyzed samples have exhibited similar features as just discussed.

III. TRANSPORT MEASUREMENTS

In a typical experiment for the measurement of classical Coulomb drag, a pair of parallel two-dimensional layers is spatially close each other but electrically separated. When one of them is current biased, a voltage drop is measured on the other one, giving rise to a finite longitudinal resistance. This effect of mutual interaction between two separated electron gases was first discussed theoretically by Price,[15] and subsequently observed in various experiments on semiconducting heterostructures.[16,17] It has been ascribed to momentum and energy exchange between the two electron gases.[18] Current drag in the presence of a magnetic field has also been investigated.[19] In fact, when a magnetic field is applied perpendicularly to the film plane, a transverse voltage arises and a Hall transresistance can be evaluated.[20] Moreover, the Coulomb interaction between two noncontacting materials has been theoretically studied for both materials in the superconducting state,[21] as well as observed between a superconductor and a normal metal separated by a thin insulating barrier.[22] Hereafter, we will present the results obtained from the experimental study of this cross-talk effect taking place in our samples between the top (superconducting) and the bottom (ferromagnetic) layers, which are electrically separated by means of an insulating (antiferromagnetic) barrier. The insertion of a ferromagnetic material introduces a new feature in the phenomenon since a spin-polarized component of transport has to be taken into account.[23] The experimental configuration used in this work is a cross geometry in which a current is sent through one of the layers and a voltage drop is measured on the other one. In Fig. 5 the bias current I_{YBCO} sent through the YBCO film is reported as a function of the voltage drop V_{LCMO} measured by separate contacts on the LCMO at $T=4.2$ K and zero applied field. The main finding is that for any given bias current, the voltage drop measured on the top side of the trilayer is reduced by increasing the barrier thickness. Such behavior is confirmed by analyzing the differential transresistance $\frac{dV_{LCMO}}{dI_{YBCO}}$ as shown in Fig. 6 at a representative voltage of 0.15 V for the three different thickness barriers.

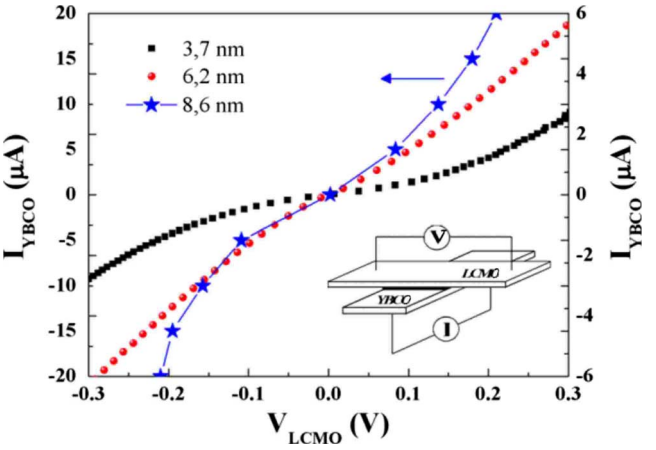

FIG. 5. (Color online) the bias current I_{YBCO} sent through the YBCO film is reported as a function of the voltage drop V_{LCMO} measured by separate contacts on the LCMO film at $T=4.2$ K and zero applied field. The inset shows the contact configuration used for the measurement on the trilayer.

When a magnetic field is applied perpendicularly to the plane of the film, the *I-V* characteristics are modified depending on the thickness of the barrier as shown in Fig. 7 for two of our samples. A peculiar behavior is observed for each case: the differential transresistance exhibits an amplitude reduction when the applied field ranges from 0 to 5 T, as indicated in Fig. 8 for samples 3 and 5 at $T=4.2$ K and for a given representative value of the voltage (0.15 V).

The case is different when the LCMO layer is current biased while the voltage drop is measured on the YBCO layer. The result is shown in Fig. 9, where one can see that no voltage drop is measured across the YBCO film below a bias current threshold of about 5 mA. The application of the magnetic field does not significantly modify the *I-V* characteristics; the response to a magnetic field in this configuration indicates no substantial change in the voltage drop as reported in Fig. 9.

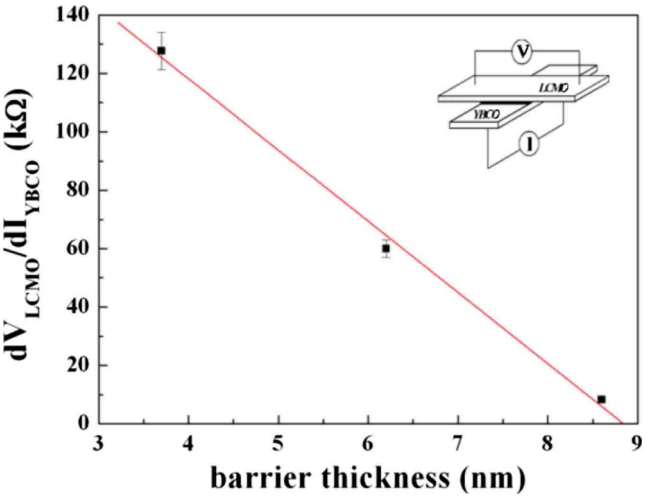

FIG. 6. (Color online) Transresistance as a function of the barrier thickness at a given value of the applied voltage for a configuration with bias current I_{YBCO} sent through the YBCO film. The line is a fit of the data.

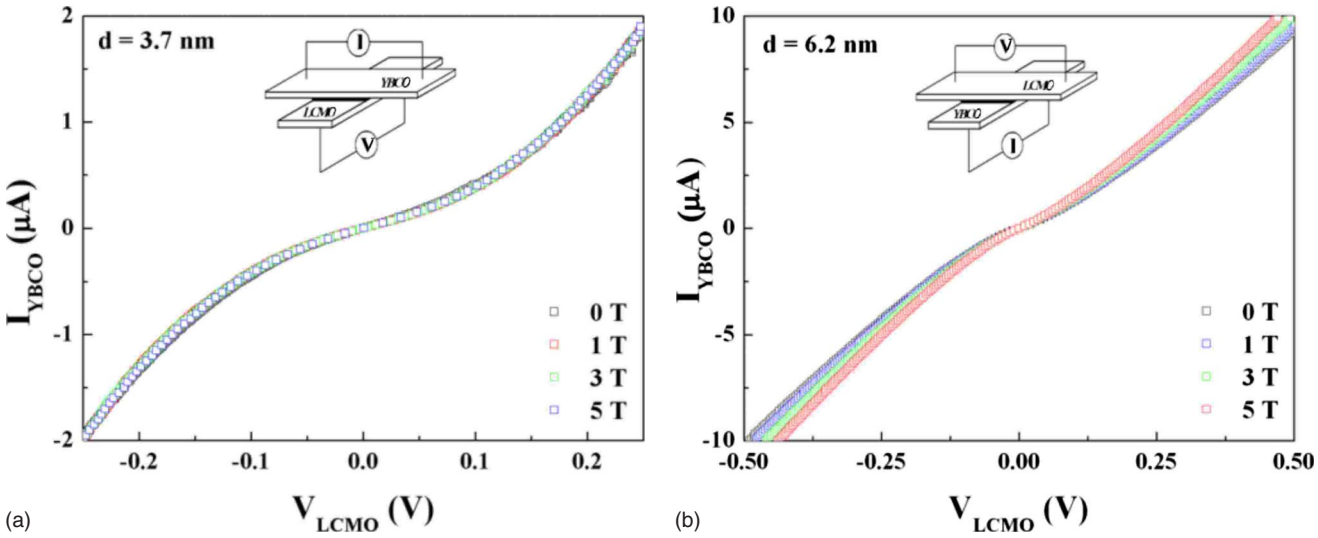

FIG. 7. (Color online) the bias current I_{YBCO} sent through the YBCO film is reported as a function of the voltage drop V_{LCMO} measured by separate contacts on the LCMO at $T=4.2$ K for different values of the applied magnetic field. The amplitude of the barrier thickness is (a) 3.7 and (b) 6.2 nm, respectively.

IV. DISCUSSION

Before commenting on the microscopic aspects involved in the observed nonlocal voltage effects, it is useful to consider a phenomenological approach that takes into account both tunneling injection and drag correlations between electrons on the ferromagnetic and the superconducting sides of the junction. Doing so, one can separately analyze the contribution arising from the tunneling with respect to that originated from the drag.[24] For the geometry of the transport measurements we have two subsystems, whose one carries current I (the drive thin film, indicated below as side 1) due to an applied voltage V while at the contacts put on the other side (indicated as part 2) there occurs an induced voltage V_i. The variable that contains the information of such nonlocal voltage effect is the so-called transresistivity ρ_D. If the two subsystems are well separated, the phenomenon is completely associated with an interlayer drag due to the friction between the two electron liquids as widely discussed in literature. However, for small barrier thickness the effect can also be influenced by the tunneling, therefore it is helpful to consider the interplay between the two mechanisms for properly interpreting the observed results. A general approach for investigating the behavior of the in-plane current densities $j_1(r)$ and $j_2(r)$ on the coordinate $r=(x,y,z)$ is based on the application of the continuity equation to the coupled thin films. If $j_t(r)$ is the tunneling current between the two subsystems, the current densities $j_1(r)$ and $j_2(r)$ can be related by a coupled set of continuity equations,[24]

$$\nabla \cdot j_1(r) + j_t(r) = 0,$$

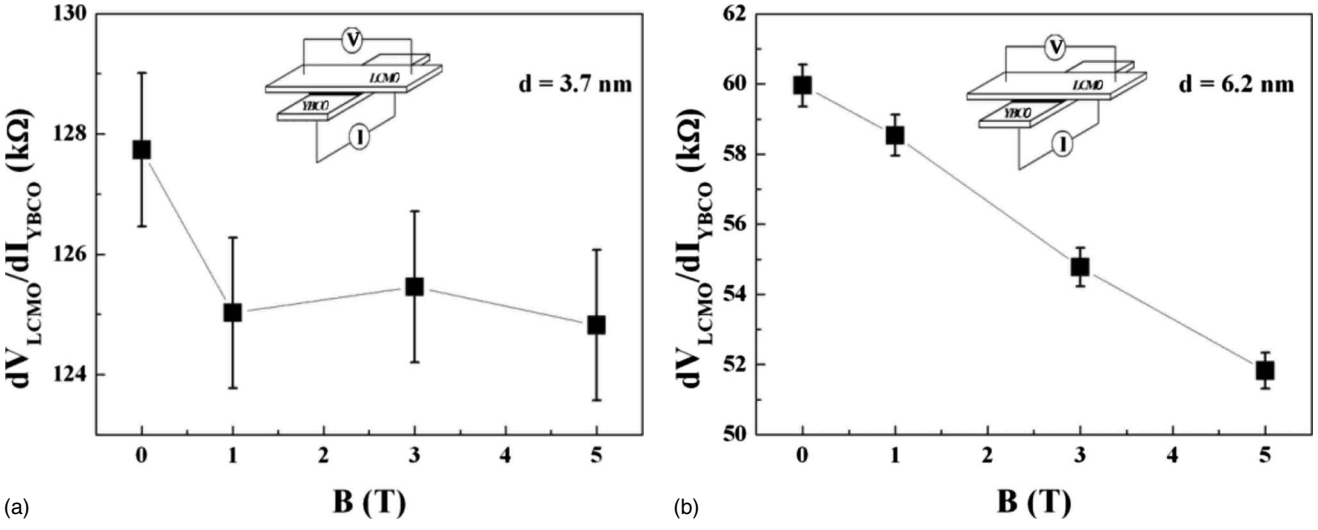

FIG. 8. Differential transresistance reported as a function of the applied magnetic field for the sample with (a) 3.7 nm and b) 6.2 nm thick barrier at a given value of the voltage. The contact configuration is such that the bias current I_{YBCO} flows through the YBCO film and the voltage drop V_{LCMO} is measured by separate contacts on the LCMO.

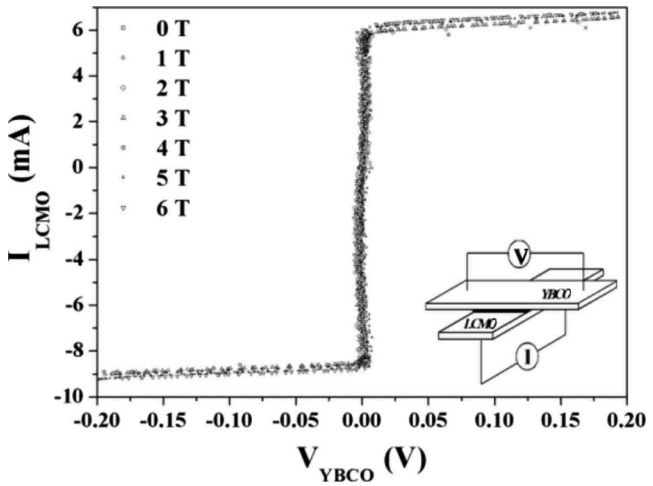

FIG. 9. The bias current I_{LCMO} sent through the LCMO film is reported as a function of the voltage drop V_{YBCO} measured by separate contacts on the YBCO film at $T=4.2$ K and zero applied field. The inset shows the contact configuration put on the trilayers as used for the measurement. The amplitude of the barrier thickness is 3.7 nm.

$$\nabla \cdot j_2(r) - j_t(r) = 0.$$

In the linear response, the current densities and the tunneling currents can be expressed via the electrochemical potentials in the two sides, $v_1(r)$ and $v_2(r)$ and to their spatial variations as follows:

$$j_t(r) = \sigma_t[v_1(r) - v_2(r)]$$

$$j_1(r) = -\sigma_1 \nabla \cdot v_1(r) - \sigma_d \nabla \cdot v_2(r)$$

$$j_2(r) = -\sigma_d \nabla \cdot v_1(r) - \sigma_2 \nabla \cdot v_2(r),$$

here σ_t is the tunneling conductance, σ_1 and σ_2 are the in-plane conductivities for the thin films, and σ_d is the transconductivity due to the frictional drag. By solving the continuity equations with the proper boundary conditions for the current and the voltage at the edge of the subsystems 1 and 2, and assuming for simplicity a geometry with parallel layers, one can obtain the expression for the transresistivity as a function of the tunneling and drag conductances,[24]

$$\rho_D = \gamma\left[\frac{(\sigma_1+\sigma_d)(\sigma_2+\sigma_d)}{(\sigma_1\sigma_2-\sigma_d^2)}\frac{2}{\kappa L}\tanh\left[\frac{\kappa L}{2}\right]-1\right]$$

with $\gamma=\frac{1}{\sigma_1+\sigma_2+2\sigma_d}$, $\kappa=\sqrt{\sigma_t(\frac{1}{\sigma_1}+\frac{1}{\sigma_2})}$, and L as the length of the subsystems. Hence, the expression for ρ_D summarizes the information on the interplay between the tunneling and the drag contributions. At this point, it is useful to consider the qualitative changes that undergo the transresistance as a function of the tunneling and the drag conductance at given values of σ_1 and σ_2. The main aspect to deduce from the expression of ρ_D is that the transresistance is a decreasing (increasing) function of the tunneling (drag) conductance amplitude σ_t (σ_d), respectively. Thus for suitable values of the parameters it might have a nonmonotonic behavior due to the interplay between the tunneling injection and the frictional drag. Such simple observations, in the framework of the above phenomenological model, permit to identify the role of the drag in the measurements of the transresistance versus the barrier thickness. Indeed, it is well accepted that the change in the barrier thickness affects the tunneling conductance because it depends exponentially on the barrier depth through the transmission coefficient. Hence, if the nonlocal voltage effects were dominated by the tunneling conductance, the transresistance would increase with the growth of the barrier size (the tunneling conductance is suppressed). The opposite observation of a reduction in the transresistance points to an explicit contribution of the frictional drag between the electrons in the superconducting and ferromagnetic side that in turn becomes more significant as the isolation of the two subsystems is enhanced or the tunneling is hindered.

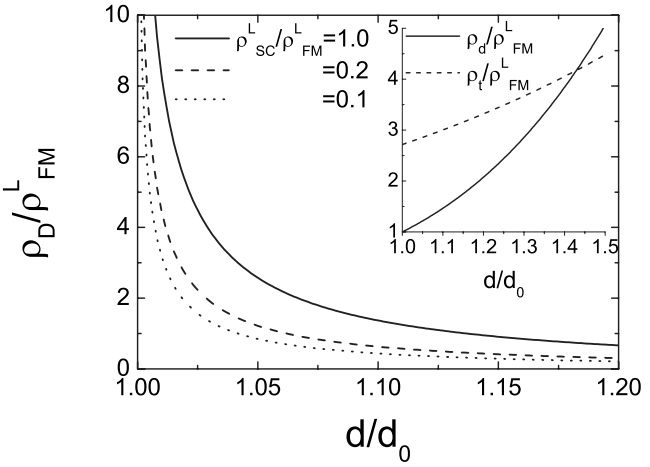

FIG. 10. Evolution of the transresistance as a function of the barrier thickness by choosing a proper parameterization for the tunneling and the drag conductance as reported in the inset.

To make the discussion more quantitative we have analyzed the transresistance in a regime that is appropriate to interpret the data. Two are the features we want to address: (i) the monotonic decrease as a function of the barrier thickness, (ii) the order of magnitude of the transresistance if compared to the resistance of the FM layer. To have a considerable enhancement of the transresistance the system has to be in the limit of $\rho^L_{\mathrm{SC}}\cdot\rho_{\mathrm{FM}}\approx\rho_d^2$ where ρ^L_{SC} and ρ^L_{FM} are the resistance for the superconducting and ferromagnetic layers, while ρ_d is the drag resistance. We have modeled the barrier thickness dependence of the tunneling and the drag conductance as $\sigma_t=\sigma_{0t}\exp[-\alpha_t\frac{d}{d_0}]$ and $\sigma_d=\sigma_{0d}\frac{1}{(d/d_0)^4}$.[25] Here, d_0, σ_{0d}, σ_{0t}, and α_t have been fixed in a way that the condition $\rho^L_{\mathrm{SC}}\cdot\rho^L_{\mathrm{FM}}=\rho_d^2$ is satisfied at $d=d_0$. d_0 is used to parameterize the behavior of the transresistance. For convenience, all the terms in the analysis have been expressed in terms of the layer resistance of the FM subsystem. In Fig. 10 the evolution of the transresistance has been reported versus the barrier thickness as compared to the layer resistance of the FM component at different values of the ratio between the superconducting and ferromagnetic layer resistance. As one can notice, the transresistance is a monotonically decreasing function of the barrier thickness and its amplitude at a given

value of d is suppressed if the layer resistance of the superconducting side gets smaller with respect to that of the ferromagnetic part.

At this point, one can also understand the similar qualitative behavior observed for the transresistance in the presence of an external field. As we have noticed in Sec. III, ρ_D is suppressed via the application of a magnetic field, and at about $B=5$ T it reduces by a factor of $\sim 13\%$ for sample 5 and of 1% for sample 3. Due to the spin polarizing effect of the field, by increasing the magnetic field it is possible to further reduce the single electron tunneling from the ferromagnet to the superconductor as a singlet-type pairing occurs in the superconducting side. Such effect on the quasiparticle injection, due to the enhancement of the ferromagnetic correlations in proximity of the insulating antiferromagnetic barrier, implies a reduction in the spin tunneling conductance if compared to the channel of the frictional drag.

At the end of such phenomenological analysis, we may conclude that the behavior of the observed nonlocal resistance has to be attributed to an interplay between the tunneling and the frictional drag contributions in the coupling between the superconducting and the ferromagnetic systems. Looking into more details, few qualitative aspects of the observed phenomena need attention. Indeed, an important point to be addressed refers to the directionality of the induced voltage in the superconducting and ferromagnetic subsystem as well as the asymmetry observed in the effect when the contacts for the bias current and the voltage drop are interchanged.

So far, we have just indicated that if a current flows in the superconducting side, it can induce along the same direction a current (thus a voltage) through the Coulomb drag or the tunneling driving charge/spin imbalance in the secondary ferromagnetic part, or vice versa. Here, the presented experimental observations are for a geometrical configuration where an induced current is perpendicular to that of the bias, thus requiring an additional mechanism for a charge/spin imbalance similar to that in transverse Hall configuration. In this frame, one should also be able to address the asymmetric behavior observed in the nonlocal resistance when the current-voltage contact configuration is interchanged. Indeed, if we start from the case of a drive current flowing within the superconducting subsystem, two mechanisms are at work. (i) The frictional drag can induce a spin current along the same direction because it is effective in the charge channel, thus it can couple to the majority-spin electron component of the half-metallic ferromagnet. (ii) The tunneling from the superconductor to the ferromagnet can couple either to the pair condensate or to the quasiparticles. Concerning the coupling with the quasiparticles, only electrons with the same spin polarization of the ferromagnet can tunnel into the ferromagnetic side due to its half-metallic behavior. Furthermore, at low temperature the quasiparticle channel is not the dominant component with respect to the pair condensate. As far as the condensate is concerned, an up electron can tunnel from the condensate into the ferromagnet at one position, via a mechanism similar to the cotunneling, and then be reabsorbed coherently at a different place on the size of the coherence length, inducing a net spin flow in the direction of the current bias. Invoking a possible spin-orbit coupling in the ferromagnet, one would then have a net spin accumulation in the direction perpendicular to the current bias. In conclusion, we see that in the configuration of a current bias in the superconductor both the drag and the tunneling contributions are effective.

Considering the case of a current flowing in the ferromagnetic subsystem and an induced voltage in the superconductor, one can notice that there are differences emerging with respect to the previous analysis. Indeed, the current in the ferromagnet can induce a charge imbalance in the superconducting side but the effect is dominated by the coupling between the spin polarized bias current and the condensate. The drag channel is unable to carry along the pairs in the condensate as it cannot coherently bring the spin-up and -down components of the electron singlet pair. Otherwise, the tunneling is similar to the case mentioned before, but now the induced current is both spin neutral (dominated by pairs) and coherent, thus no transverse voltage effect is observed (see Fig. 9). When the current bias overcomes a critical threshold, the quasiparticle component in the superconductor is enhanced due to the pair breaking induced through the drag and the spin tunneling. The resulting net spin current induced in the superconductor can then be deflected by mechanisms of side jump or skew scattering in analogy to those observed in similar spin injection configurations.[26]

Another important aspect concerns with the role of the proximity effect close to the interface and the magnetization profile in the FM side. If the magnetization of LCMO layers close to the interface is not in the half-metallic regime and the electrons lose their spin orientation approaching the interface, then the proximity between the SC and the FM components is modified, and the electrons have a probability of charge transfer from the SC to the FM part in both spin channels. This implies an increase in the barrier conductance with respect to the "ideal" case where only a single spin channel of injection is active. Moreover, for this circumstance the superconducting fluctuations due to pair leaking in the weakly polarized FM layers close to the interface can reduce the intralayer resistance. The net effect is to modify quantitatively both the barrier conductance and the resistance of the FM part. Both effects, according to our analysis, would tend to increase the transresistance. In the same spirit of the previous discussion, we can consider the role of Andreev reflections close to the interface. Basically, they turn out to influence quantitatively the barrier conductance in a direct way, while the modifications on the drag conductance as well as on the intralayer conductivities are more subtle to be accounted. At the lowest level of description, one can focus on the changes induced in the barrier conductance. In particular, concerning the role of Andreev processes we do expect that their effect on the transresistance appears via the modification of the barrier conductance and in turn to the tunnel contribution. In this framework, it is known that Andreev reflections can play an important role in high transparent ferromagnet-superconductor heterostructures. Andreev bound states induce a zero-bias peak in the conductance and are observed in the a-b plane tunneling experiments for d-wave superconductors. Such bound states are suppressed in presence of a strong spin polarization. In ideal c-axis oriented junctions, one does not expect to observe zero-bias

peak in the conductance. However, due to the interfacial roughness of optimally grown YBCO, *a-b* plane processes may contribute to the *c*-axis transport thus giving access to zero-bias conductance peak also in the *c*-axis geometry. Then, also in this case, it is possible to observe the reduction in the zero-bias conductance peak by the spin-polarized transport across the interface. Thus we expect that Andreev processes for the LCMO-F/LCMO-AF/YBCO junction may modify the barrier conductance if the FM is not in the half-metallic regime otherwise they are usually suppressed. Both cases can be directly included by properly parameterizing the amplitude of the tunneling conductance.

V. CONCLUSIONS

In conclusion, we have succeeded in fabricating epitaxial trilayers in cross configuration constituted by a LCMO-half-metal ferromagnet and a YBCO-superconductor separated by an insulating barrier of LCMO antiferromagnet having different thickness. To investigate some unusual features emerging from the interaction between the superconductor and the ferromagnet, we have looked at nonlocal conductance effects by applying a drive current on one side of the trilayer and searching for an induced voltage drop at the edge of the other part of the system. The observed transresistance exhibits a nontrivial dependence on the barrier thickness size as well as on the magnetic field that we have interpreted as an interplay between tunneling and drag effects between the superconducting and ferromagnetic subsystems. The obtained results have distinctive qualitative features as the asymmetric behavior observed by interchanging the current-voltage contact configurations. Such observation reveals how the spin/charge injection as well as the imbalance induced by the drag mechanism is strongly interrelated to the nature of the pair condensate and to the presence of a half-metallic ferromagnet. Further studies in this direction are in progress to clarify the intrinsic nature and the microscopic components contributing to the nonlocal conductance for the trilayer system upon examination.

[1] A. Buzdin, Rev. Mod. Phys. **77**, 935 (2005).
[2] F. S. Bergeret, A. F. Volkov, and K. B. Efetov, Rev. Mod. Phys. **77**, 1321 (2005).
[3] A. F. Volkov, F. S. Bergeret, and K. B. Efetov, Phys. Rev. Lett. **90**, 117006 (2003).
[4] M. Eschrig, J. Kopu, J. C. Cuevas, and Gerd Schon, Phys. Rev. Lett. **90**, 137003 (2003).
[5] R. S. Keizer, S. T. B. Goennenwein, T. M. Klapwijk, G. Miao, G. Xiao, and A. Gupta, Nature (London) **439**, 825 (2006).
[6] T. Kontos, M. Aprili, J. Lesueur, F. Genet, B. Stephanidis, and R. Boursier, Phys. Rev. Lett. **89**, 137007 (2002).
[7] J. W. A. Robinson, S. Piano, G. Burnell, C. Bell, and M. G. Blamire, Phys. Rev. Lett. **97**, 177003 (2006).
[8] V. A. Vas'ko, V. A. Larkin, P. A. Kraus, K. R. Nikolaev, D. E. Grupp, C. A. Nordman, and A. M. Goldman, Phys. Rev. Lett. **78**, 1134 (1997).
[9] C. A. R. Sa de Melo, Phys. Rev. Lett. **79**, 1933 (1997).
[10] D. Sanchez, R. Lopez, P. Samuelsson, and M. Buttiker, Phys. Rev. B **68**, 214501 (2003).
[11] P. Cadden-Zimansky, Z. Jiang, and V. Chandrasekhar, New J. Phys. **9**, 116 (2007).
[12] E. Baca, W. Saldarriaga, J. Osorio, G. Campillo, M. E. Gomez, and P. Prieto, J. Appl. Phys. **93**, 8206 (2003).
[13] Y. X. Wang, Y. Du, R. W. Qin, B. Han, J. Du, and J. H. Lin, J. Solid State Chem. **156**, 237 (2001).
[14] *X-ray Scattering From Semiconductors*, edited by P. F. Fewster (Imperial College Press, PANalytical Research Centre, UK, 2003).
[15] P. J. Price, in *The Physics of Submicron Semiconductor Devices*, edited by H. Grubin, D. K. Ferry, and C. Jacoboni (Plenum, New York, 1988), p. 445.
[16] P. M. Solomon, P. J. Price, D. J. Frank, and D. C. La Tulipe, Phys. Rev. Lett. **63**, 2508 (1989).
[17] T. J. Gramila, J. P. Eisenstein, A. H. MacDonald, L. N. Pfeiffer, and K. W. West, Phys. Rev. Lett. **66**, 1216 (1991).
[18] A. G. Rojo, J. Phys.: Condens. Matter **11**, R31 (1999).
[19] H. C. Tso and P. Vasilopoulos, Phys. Rev. B **45**, 1333 (1992).
[20] Y. Oreg and B. I. Halperin, Phys. Rev. B **60**, 5679 (1999).
[21] J.-M. Duan and S. Yip, Phys. Rev. Lett. **70**, 3647 (1993).
[22] N. Giordano and J. D. Monnier, Phys. Rev. B **50**, 9363 (1994).
[23] I. D'Amico and G. Vignale, Phys. Rev. B **62**, 4853 (2000).
[24] O. E. Raichev, J. Appl. Phys. **81**, 1302 (1997); O. E. Raichev and F. T. Vasko, Phys. Rev. B **55**, 2321 (1997).
[25] T. G. Gramila, J. P. Eisenstein, A. H. MacDonald, L. N. Pfeiffer, and K. W. West, Phys. Rev. Lett. **66**, 1216 (1991).
[26] S. Takahashi and S. Maekawa, Phys. Rev. Lett. **88**, 116601 (2002); S. Takahashi and S. Maekawa, Physica C **437-438**, 309 (2006).